PAPER • OPEN ACCESS

Dephasing–rephasing dynamics of one-dimensional tunneling quasicondensates

To cite this article: A Tononi *et al* 2020 *New J. Phys.* **22** 073020

View the article online for updates and enhancements.

New Journal of Physics

The open access journal at the forefront of physics

Deutsche Physikalische Gesellschaft **DPG**

IOP Institute of Physics

Published in partnership with: Deutsche Physikalische Gesellschaft and the Institute of Physics

Dephasing–rephasing dynamics of one-dimensional tunneling quasicondensates

A Tononi[1,4] , F Toigo[1] , S Wimberger[2,3] , A Cappellaro[1] and L Salasnich[1]

1   Dipartimento di Fisica e Astronomia 'Galileo Galilei', Università di Padova, via Marzolo 8, 35131 Padova, Italy
2   Dipartimento di Scienze Matematiche, Fisiche ed Informatiche, Università di Parma, Parco Area delle Scienze 7/A, 43124 Parma, Italy
3   INFN, Sezione di Milano Bicocca, Gruppo Collegato di Parma, Parma, Italy
4   Author to whom any correspondence should be addressed.

E-mail: andrea.tononi@phd.unipd.it

Abstract

We study the quantum tunneling of two one-dimensional quasi-condensates made of alkali-metal atoms, considering two different tunneling configurations: side-by-side and head-to-tail. After deriving the quasiparticle excitation spectrum, we discuss the dynamics of the relative phase following a sudden coupling of the independent subsystems. In particular, we calculate the coherence factor of the system, which, due to the nonzero tunneling amplitude, it exhibits dephasing–rephasing oscillations instead of pure dephasing. These oscillations are enhanced by a higher tunneling energy, and by higher system densities. Our predictions provide a benchmark for future experiments at temperatures below $T \lesssim 5\,\mathrm{nK}$.
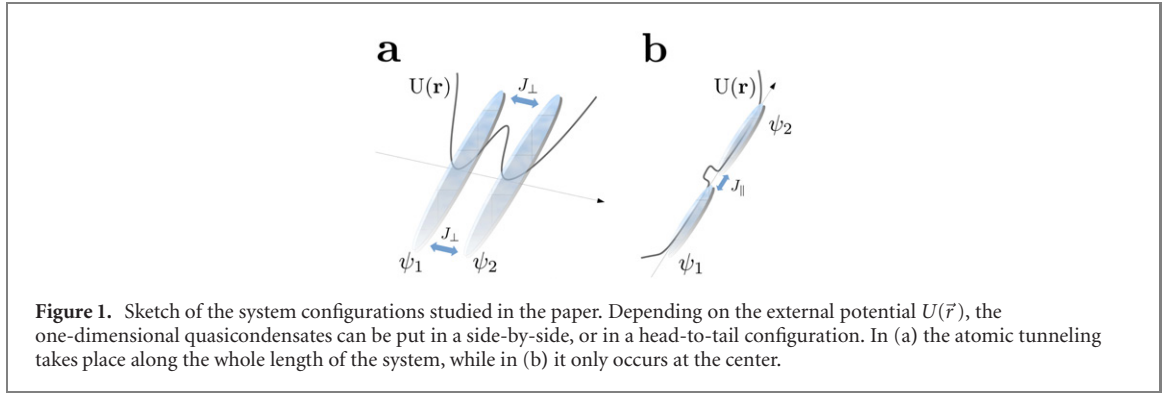
1. Introduction

The interference of incoherent waves and the emergence of beats are fundamental physical phenomena, which can be observed both in classical and in quantum systems. Due to their high coherency, and for the reduced occupation of excited states, atomic Bose–Einstein condensates (BECs) are an ideal platform to study the dephasing and resynchronization of noninteracting modes with commensurate frequencies.

Indeed, since their first experimental realization [1, 2], BECs have represented a paradigmatic setup to probe the dynamics of macroscopic quantum observables. Besides being one of the hallmarks of the transition, phase coherence is the key property one aims to preserve and it is an ongoing issue for quantum technologies and devices [3–5]. Thus, the question of how long coherence can be sustained is relevant for practical applications. At the same time, the qualitative and quantitative understanding of the concept of phase coherence addresses a fundamental problem of many body systems made of interacting constituents [6].

The first theoretical analyses on this topic were devoted to the investigation of the tunneling dynamics between independently-formed condensates [6–8]. By drawing an electrostatic analogy, an effective (semiclassical) theory can effectively describe the Josephson tunneling between the two atomic systems [7, 9]. A refined description in terms of quasiparticles can also account for damped oscillations and eventual decoherence effects due to the presence of an external potential [10, 11].

Throughout the last two decades, key advancements have been obtained by focusing on atomic interferometers in lower dimensionalities, and adopting refined field-theoretical techniques [15–23]. Following these works, we consider the paradigmatic experimental setup of a pair of one-dimensional parallel quasicondensates [12, 13]. This configuration is produced by a fast and coherent splitting of a single superfluid with radiofrequency-induced adiabatic potentials [14, 15]. Some notable works on this configuration have also shown the emergence of a prethermalized stationary state during the relaxation of the closed system [24–27].

Here we discuss the out-of-equilibrium dynamics of parallel quasicondensates in which, after the initial splitting, a nonzero tunneling between the subsystems is restored. In this context, recent works have

Figure 1. Sketch of the system configurations studied in the paper. Depending on the external potential $U(\vec{r})$, the one-dimensional quasicondensates can be put in a side-by-side, or in a head-to-tail configuration. In (a) the atomic tunneling takes place along the whole length of the system, while in (b) it only occurs at the center.

analyzed the role of a Josephson coupling between the parallel superfluids, considering in particular the rephasing dynamics [28, 29] and the relaxation of the system [30] after a quench of the tunneling energy. Interestingly, a recent experiment has found a relaxation of the Josephson oscillations to a phase-locked equilibrium state [31], an effect which may crucially depend on the harmonic confinement [32, 33]. In our paper, we investigate both the usual experimental configuration of side-by-side parallel quasicondensates with uniform tunneling (figure 1(a)), and the arrangement of head-to-tail parallel superfluids with a delta-like Josephson junction (figure 1(b)) [34]. In both configurations, due to the similar structure of the quasiparticle energy, we find that the coherence factor oscillates in time, proving the partial decoherence and resynchronization of the noninteracting modes of the coupled quasicondensates. This phenomenon is the outcome of the competition between the quantum fluctutations of the single quasicondensates, and the coherence-inducing Josephson coupling, which introduces a mass gap in the quasiparticle spectrum. Previous works on side-by-side superfluids did not predict explicitly the oscillations of the coherence factor [30], and our work analyzes the configuration of head-to-tail quasicondensates for the first time. The experimental observation of these phase oscillations requires a low initial temperature of the quasicondensate ($\sim$ nK range), to avoid the intrinsic dephasing induced by thermal fluctuations.

The paper is organized as follows: in section 2 we introduce our model for parallel quasicondensates. Then, we reformulate the dynamics of the relative variables in terms of quasiparticle excitations in section 3, considering both the head-to-tail and the side-by-side system configurations. Finally, section 4 explores the phase dynamics of the parallel superfluids after a quench in the tunneling amplitude.

2. The model and the relative dynamics

In systems of ultracold atoms the tunneling dynamics is strongly dependent on the specific configuration and on the spatial dimension, i.e. on the details of the confining potential $U(\vec{r})$. Here we discuss the phase dynamics of one-dimensional tunneling quasicondensates, which are obtained by confining the atoms with radiofrequency-induced adiabatic potentials [14, 15]. By properly tuning the trap parameters and the radiofrequency field detuning, parallel condensates can be prepared either in a side-by-side, or in a head-to-tail configuration. In both cases, we describe each one-dimensional superfluid with the complex-valued field $\psi_j(x, t)$, where $j = 1, 2$ labels each subsystem, x is the coordinate in the longitudinal direction, and t is time.

The real-time Lagrangian L of the system can be written as

$$L = \int_0^L \mathrm{d}x \mathcal{L}, \quad \mathcal{L} = \mathcal{L}_{\mathrm{tun}} + \sum_{j=1,2} \mathcal{L}_{0,j}. \tag{1}$$

Here $\mathcal{L}_{0,j}$ is the Lagrangian density of the uncoupled quasicondensates, namely

$$\mathcal{L}_{0,j} = \mathrm{i}\hbar \psi_j^* \partial_t \psi_j - \frac{\hbar^2}{2m} |\partial_x \psi_j|^2 - \frac{g}{2} |\psi_j|^4, \tag{2}$$

where m is the mass of each atom, g is the one-dimensional interaction strength [35], and $\hbar$ is the reduced Planck constant. Note that in our effective one-dimensional approach we omit the external potential, assuming that the transverse degrees of freedom are not excited. Moreover, in the absence of a longitudinal potential, the atomic density along x will be approximately uniform. The Lagrangian density $\mathcal{L}_{\mathrm{tun}}$ in

equation (1) describes the tunneling of atoms between the two superfluids, namely

$$\mathcal{L}_{\text{tun}} = \frac{J}{2}\left(\psi_1^* \psi_2 + \psi_2^* \psi_1\right),\tag{3}$$

where the specific expression of the tunneling energy $J \equiv J(x)$ depends on the configuration considered. In the side-by-side configuration (figure 1(a)) we express it as $J = J_\perp$, with $J_\perp$ uniform and constant. In the head-to-tail configuration (figure 1(b)) we choose $J = 2J_\parallel L\,\delta(x)$, since tunneling will occur only at the origin of the system[4].

To describe the hydrodynamic properties of the system, we rewrite the complex field as $\psi_j(x,t) = [\rho_j(x,t)]^{1/2} e^{i\phi_j(x,t)}$, where $\rho_j(x,t)$ is the local density of the bosonic atoms in the subsystem j and $\phi_j(x,t)$ is the phase angle [36]. Substituting this field parametrization into the Lagrangian density of equation (1), we find

$$\mathcal{L} = \sum_{j=1,2}\left[-\hbar\rho_j\dot{\phi}_j - \frac{\hbar^2\rho_j}{2m}(\partial_x\phi_j)^2 - \frac{\hbar^2}{8m\rho_j}(\partial_x\rho_j)^2 - \frac{g}{2}\rho_j^2\right] + J\sqrt{\rho_1\rho_2}\,\cos(\phi_1 - \phi_2).\tag{4}$$

The tunneling dynamics, as can be seen from the last term of equation (4), is triggered by a nonzero relative phase $\phi_1 - \phi_2$ between the superfluids: our goal is to derive an effective Hamiltonian description of the relative phase dynamics. Indeed, phase correlators are the main observable quantities in cold atom interferometry and decoherence experiments [13, 26, 37]. We thus define the total phase $\bar{\phi}$ and relative one ϕ as

$$\bar{\phi} = \phi_1 + \phi_2, \quad \phi = \phi_1 - \phi_2,\tag{5}$$

and we define the total density $\bar{\rho}$ and the density imbalance ζ as

$$\bar{\rho} = \frac{\rho_1 + \rho_2}{2}, \quad \zeta = \frac{\rho_1 - \rho_2}{2\bar{\rho}}.\tag{6}$$

After these new variables are substituted in equation (4), different terms will appear in the new Lagrangian density: those which contain only the total (or center of mass) fields, those of the relative fields, and the couplings between relative and total fields. The latter terms can be neglected under the assumption that the total density takes the mean field value of $\bar{\rho}(x,t) = \bar{\rho}$, namely that the fluctuations of the total density are negligible, and assuming a uniform and constant value of $\bar{\phi}$. If the couplings between total and relative modes are neglected, we can focus only on the Lagrangian density of the relative modes $\mathcal{L}_{\text{rel}}$, which reads

$$\mathcal{L}_{\text{rel}} = -\hbar\bar{\rho}\zeta\dot{\phi} - \frac{\hbar^2\bar{\rho}}{4m}(\partial_x\phi)^2 - \frac{\hbar^2\bar{\rho}}{4m}\frac{(\partial_x\zeta)^2}{1-\zeta^2} - g\bar{\rho}^2\zeta^2 + J\bar{\rho}\sqrt{1-\zeta^2}\,\cos(\phi).\tag{7}$$

By considering only the relative fields, we are neglecting in particular the anharmonic terms which couple the density fluctuations with the phase modes. These contributions are unimportant in the zero-temperature quantum regime that we consider [17], but can have a relevant role in the dynamics of a system at a finite temperature [17], and for zero interaction between the subsystems [38, 39]. In this regard, a discussion of the validity of our scheme for the typical experimental parameters will be given in the conclusions.

Our Lagrangian, equation (7), extends the usual two-mode description of quantum tunneling by including the contribution of the longitudinal excitations of the system. This is particularly evident from the Euler–Lagrange equations for equation (7), which read

$$\hbar\dot{\phi} = -J\frac{\zeta}{\sqrt{1-\zeta^2}}\,\cos(\phi) - 2g\bar{\rho}\zeta + \frac{\hbar^2}{2m}\left[\frac{\partial_x^2\zeta}{1-\zeta^2} + \frac{\zeta(\partial_x\zeta)^2}{(1-\zeta^2)^2}\right],\tag{8}$$

$$\hbar\dot{\zeta} = J\sqrt{1-\zeta^2}\,\sin(\phi) - \frac{\hbar^2}{2m}\partial_x^2\phi.\tag{9}$$

These equations reproduce the Josephson–Smerzi equations [40, 41] for bosons in a double well potential if $J = J_0$, with J_0 uniform and constant, and the spatial dependence of the fields is removed. At the same time, our equations (8) and (9) describe the complex dynamics in which the tunneling of the zero momentum mode couples with the Bogoliubov excitations of the superfluids.

In the linear regime, for a small amplitude of the relative phase field and of the imbalance, equations (8) and (9) can be simplified as

---

[4] Strictly speaking, in the head-to-tail configuration the superfluid with label 1 occupies the region $-L \leqslant x \leqslant 0$. The invariance under reflection of x in $-x$ of $\mathcal{L}_{0,j}$ allows to write equation (1).

$$\hbar\dot{\phi} = -(J + 2g\bar{\rho})\,\zeta + \frac{\hbar^2}{2m}\partial_x^2\zeta, \tag{10}$$

$$\hbar\dot{\zeta} = J\phi - \frac{\hbar^2}{2m}\partial_x^2\phi. \tag{11}$$

These equations can be obtained as the Euler–Lagrange equations of the following low-energy effective Lagrangian

$$\mathcal{L}_{\mathrm{rel}} = -\hbar\bar{\rho}\,\zeta\dot{\phi} - \frac{\hbar^2\bar{\rho}}{4m}(\partial_x\phi)^2 - \frac{\hbar^2\bar{\rho}}{4m}(\partial_x\zeta)^2 - \frac{(2g\bar{\rho}^2 + J\bar{\rho})}{2}\zeta^2 - \frac{J\bar{\rho}}{2}\phi^2, \tag{12}$$

which is quadratic in the relative fields.

3. Reformulation in terms of quasiparticles

In this section, we derive the excitation spectrum of the coupled superfluids in the side-by-side configuration, and in the head-to-tail one. For both configurations, we reformulate the complex dynamics of interacting tunneling quasicondensates in terms of noninteracting quasiparticle excitations.

3.1. Side-by-side parallel quasicondensates
To describe the side-by-side tunneling configuration (figure 1(a)), we consider a uniform and constant tunneling energy $J = J_\perp$. Let us introduce the Fourier representation of the relative phase $\phi(x, t)$ and of the imbalance $\zeta(x, t)$, namely

$$\phi(x, t) = \frac{\sqrt{2}}{L}\sum_{k\geqslant0}\phi_k(t)\cos(kx), \quad \phi_k(t) = \alpha_k\int_0^L \mathrm{d}x\,\phi(x, t)\cos(kx), \tag{13}$$

$$\zeta(x, t) = \frac{\sqrt{2}}{L}\sum_{k\geqslant0}\zeta_k(t)\cos(kx), \quad \zeta_k(t) = \alpha_k\int_0^L \mathrm{d}x\,\zeta(x, t)\cos(kx), \tag{14}$$

where we have imposed open boundary conditions, i.e. $\partial_x\phi(0, t) = \partial_x\phi(L, t) = 0$, $\partial_x\zeta(0, t) = \partial_x\zeta(L, t) = 0$, at any time t. The wavevector k is given by $k = \pi n/L$, with $n = 0, 1, 2, \ldots$ and we define the parameter $\alpha_k = \sqrt{2}$ for $k \neq 0$, while $\alpha_0 = 1/\sqrt{2}$.

We now substitute these Fourier field decompositions into the real space Lagrangian L_{rel} associated to the Lagrangian density $\mathcal{L}_{\mathrm{rel}}$ of equation (12). Thereafter, the Euler–Lagrange equation for ϕ_k yields an explicit expression of the imbalance mode ζ_k: substituting it in the Lagrangian L_{rel}, we get an effective Lagrangian for the phase modes only. With the usual Legendre transform, we can write the corresponding effective Hamiltonian as

$$H = \sum_k \left[\frac{p_k^2}{2M_k} + \frac{M_k}{2}\omega_k^2\phi_k^2\right], \tag{15}$$

where $p_k = M_k\dot{\phi}_k$ are the linear momenta associated to the generalized coordinates ϕ_k. In this way, we have reformulated the low-energy description of tunneling quasicondensates as a sum of noninteracting harmonic oscillators, or quasiparticles. Each oscillator has a wavevector-dependent effective mass M_k, namely

$$M_k = \frac{\hbar^2\bar{\rho}}{L}\frac{1}{(J_\perp + 2g\bar{\rho}) + \hbar^2k^2/(2m)}, \tag{16}$$

and a quasiparticle energy given by

$$\hbar\omega_k = \sqrt{J_\perp(J_\perp + 2g\bar{\rho}) + \frac{\hbar^2k^2}{2m}\left(\frac{\hbar^2k^2}{2m} + 2(J_\perp + g\bar{\rho})\right)}. \tag{17}$$

This quasiparticle energy is a gapped Bogoliubov-like spectrum, and the zero-mode term reproduces the usual Josephson tunneling energy. Indeed, for $k = 0$, the excitation energy of equation (17) reads

$$\hbar\omega_0 = \sqrt{J_\perp^2 + 2g\bar{\rho}J_\perp}, \tag{18}$$

and ω_0 is exactly the Josephson oscillation frequency in the absence of spatial dependence of the fields [41]. At the same time, in the absence of tunneling among the subsystems, i.e. setting $J_\perp = 0$, we get

$$\hbar\omega_{k,B} = \sqrt{\frac{\hbar^2 k^2}{2m}\left(\frac{\hbar^2 k^2}{2m} + 2g\bar{\rho}\right)}, \qquad (19)$$

that is the familiar Bogoliubov spectrum of elementary excitations along the longitudinal direction [42]. For small wavevectors, the Bogoliubov spectrum can be approximated by the phonon spectrum $\hbar\omega_k = c_s\hbar k$, with the speed of sound given by $c_s = (g\bar{\rho}/m)^{1/2}$. We emphasize that, in this low-energy non-tunneling regime the quasiparticle mass is wavevector independent, namely $M = \hbar^2/(2gL)$, and our procedure reproduces the results of reference [21]. Moreover, for a nonzero tunneling energy $J_\perp$ between the quasicondensates, and in the Josephson regime of $g\bar{\rho} \gg J_\perp$, our excitation spectrum of equation (17) is consistent with the one derived in references [29, 30]. With respect to these works, therefore, we obtain a more general excitation spectrum, which includes the free-particle behavior of the Bogoliubov spectrum for large wavevectors.

3.2. Head-to-tail parallel quasicondensates

In head-to-tail parallel superfluids (figure 1(b)) we model the tunneling energy as $J(x) = 2J_\parallel L\delta(x)$. We implement a low-energy effective description of this system configuration by neglecting the spatial derivatives of the imbalance in equation (10). For consistency with this approximation, we work in the Josephson regime of $g\bar{\rho} \gg J_\parallel$, in which the experiments are usually performed [31, 37]. In this case, equation (10) can be easily solved as $\zeta = -\hbar\dot{\phi}/(2g\bar{\rho})$, and, substituting it into equation (12), we get an effective Lagrangian density for the relative phase

$$\mathcal{L}_{\text{rel}} = \frac{\hbar^2}{4g}\dot{\phi}^2 - \frac{\hbar^2\bar{\rho}}{4m}(\partial_x\phi)^2 - J_\parallel\bar{\rho}L\delta(x)\phi^2. \qquad (20)$$

In analogy with the previous subsection, here we decompose the phase field as

$$\phi(x,t) = \frac{1}{\sqrt{L}}\sum_n q_n(t)\,\phi_n(x), \qquad (21)$$

where the $\phi_n(x)$ are real and orthonormal eigenfunctions of the eigenvalue problem

$$\left[-\frac{\hbar^2}{2m}\partial_x^2 + 2J_\parallel L\delta(x)\right]\phi_n(x) = \epsilon_n\,\phi_n(x); \qquad (22)$$

with open boundary conditions $\partial_x\phi_n(0) = \partial_x\phi_n(L) = 0$. The eigenvalues ϵ_n of equation (22) are determined by the following equation for ϵ

$$\sqrt{\frac{2mL^2\epsilon}{\hbar^2}}\,\tan\left(\sqrt{\frac{2mL^2\epsilon}{\hbar^2}}\right) = \frac{2mL^2 J_\parallel}{\hbar^2}, \qquad (23)$$

which admits an infinite set of solutions, labelled by the integer number n [43].

These solutions may either be obtained numerically or well approximated by the following analytical approximations, holding when $n \ll \tilde{J}_\parallel$ or $n > \tilde{J}_\parallel$, where $\tilde{J}_\parallel = J_\parallel\pi/(\hbar^2\pi^2/(2mL^2))$. First of all, in the regime of $n > \tilde{J}_\parallel$, the solutions ϵ_n of equation (23) are well approximated by

$$\epsilon_n = \frac{1}{4}\left(\sqrt{4J_\parallel + \frac{\hbar^2\pi^2 n^2}{2mL^2}} + \sqrt{\frac{\hbar^2\pi^2 n^2}{2mL^2}}\right)^2, \qquad (24)$$

which, essentially, is the energy of a free particle with a mass gap. Actually, provided that $\tilde{J}_\parallel \leqslant \pi/16$, equation (24) holds also for $n = 0$. In the opposite case of $n \ll \tilde{J}_\parallel$ the solutions of equation (23) are instead well approximated by:

$$\epsilon_n = \frac{\hbar^2\pi^2}{2mL^2}\frac{J_\parallel}{J_\parallel + \frac{\hbar^2}{2mL^2}}\left(n + \frac{1}{2}\right)^2. \qquad (25)$$

which holds also for $n = 0$ when $\tilde{J}_\parallel \geqslant 1/\pi$. Finally, we emphasize that in the intermediate range of values of $\tilde{J}_\parallel$, namely for $\pi/16 \leqslant \tilde{J}_\parallel \leqslant 1/\pi$, the lowest solution ($n = 0$) of equation (24) may be written as $\epsilon_0 = \hbar^2\pi^2/(32mL^2)$.

In analogy with the the previous subsection, we insert the decomposition of equation (21) into the effective Lagrangian density $\mathcal{L}_{\text{rel}}$ of equation (20). Then, calculating the corresponding Hamiltonian with a Legendre transformation, we get

$$H = \sum_n \left[\frac{P_n^2}{2M} + \frac{M}{2}\Omega_n^2 \phi_n^2 \right], \qquad (26)$$

where $P_n = M\dot{\phi}_n$ are generalized momenta associated to the phase modes ϕ_n. Again, we are describing the dynamics of the relative degrees of freedom for head-to-tail parallel quasicondensates as noninteracting harmonic oscillators with the effective mass $M = \hbar^2/(2gL)$, and the harmonic frequency $\Omega_n = (2g\bar{\rho}\,\epsilon_n/\hbar^2)^{1/2}$. From the knowledge of the eigenvalues ϵ_n, obtained from equation (23), one immediately derives the frequencies Ω_n. In the following section we will discuss the relative phase dynamics of this system in a regime of very small Josephson tunneling $J_\parallel$, where equation (24) is reliable even for $n = 0$. In this case, the quasiparticle energies can be expressed as

$$\hbar\Omega_k = \sqrt{2g\bar{\rho}J_\parallel + \frac{g\bar{\rho}}{2}\frac{\hbar^2 k^2}{2m}} + \sqrt{\frac{g\bar{\rho}}{2}\frac{\hbar^2 k^2}{2m}}, \qquad (27)$$

where, as in the previous subsection, we have introduced the wavevector $k = n\pi/L$.

4. Phase oscillations in one-dimensional tunneling quasicondensates

We now discuss the phase dynamics after a quantum quench of the tunneling amplitude, describing a procedure which can be implemented both for tunneling side-by-side and head-to-tail quasicondensates.

The time evolution of the relative phase and of its correlation functions is crucially dependent on the experimental protocol adopted to prepare the initial state, and on the Hamiltonian under which the system evolves. Here we suppose that the atomic system, initially confined in a one-dimensional single quasicondensate, is symmetrically split into a couple of parallel superfluids. In the experiments, the splitting procedure consists in tuning a radiofrequency field to create a double well adiabatic potential for the parallel condensates [15]. For a large enough number of atoms in the system, as argued in references [17, 21, 30], the splitting procedure leads to a Gaussian probability distribution of the imbalance, with zero mean and a variance proportional to the mean-field density $\bar{\rho}$. Hence, assuming a minimum uncertainty for the relative phase ϕ, canonically conjugated to the imbalance ζ, the initial wavefunction in the relative phase representation is given by [21]

$$\Psi[\{\phi_k\}, t=0] \simeq \prod_k \Psi_k(\phi_k, t=0), \qquad (28)$$

where the single phase wavefunction reads

$$\Psi_k(\phi_k, t=0) = \frac{1}{\pi^{1/4}\sigma^{1/2}} e^{\frac{-\phi_k^2}{2\sigma^2}}, \qquad (29)$$

with $\sigma^2 = L^2/N = L/\bar{\rho}$, since ϕ_k is dimensionally a length. Note that, in order to have small fluctuations in the relative phase field, the splitting time τ_s must be very short. In particular, τ_s must satisfy the condition of $\tau_s \ll \xi/c_s$, with $\xi = (\hbar^2/mg\bar{\rho})^{1/2}$ the healing length, and c_s the speed of sound of the single superfluid [21]. At the same time, τ_s must be long enough to avoid the excitation of the transverse modes of the one-dimensional superfluids.

Given the Gaussian initial state in terms of the phase modes ϕ_k, we want to calculate its time evolution under the harmonic Hamiltonians of the tunneling quasicondensates, namely equations (15) and (26). Experimentally, the time evolution under these Hamiltonians can be implemented by lowering the barrier which separates the superfluids. This procedure must take place in a finite but quick enough time $\tau_J \approx \tau_s$, to avoid excessive dephasing on one hand [21], and to keep the system near the initial state, equation (29), on the other.

In the Schrödinger picture, the quantum dynamics of the system of oscillators with Hamiltonians of equations (15) and (26), follows the Schrödinger equation

$$i\hbar\partial_t \Psi_k(\phi_k, t) = \left[-\frac{\hbar^2}{2M_k}\frac{\partial^2}{\partial\phi_k^2} + \frac{M_k\omega_k^2}{2}\phi_k^2 \right]\Psi_k(\phi_k, t), \qquad (30)$$

where the mass M_k and the oscillator frequency ω_k are those calculated previously in the side-by-side, and in the head-to-tail configurations. For each oscillator, the wavefunction remains Gaussian during the time evolution, but the standard deviation evolves with time. In particular, the probability density of the mode k at time t becomes [44]

$$|\Psi_k(\phi_k, t)|^2 = \frac{1}{\pi^{1/2}\sigma_k(t)} e^{-\frac{\phi_k^2}{\sigma_k^2(t)}} \qquad (31)$$
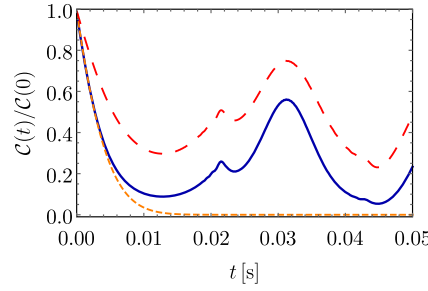
Figure 2. Recurrent dephasing–rephasing dynamics of side-by-side tunneling quasicondensates for different system lengths: $L = 50\,\mu$m (blue solid line), $L = 100\,\mu$m (red long-dashed line). Differently from uncoupled superfluids, which dephase exponentially [21] (orange dashed line), in the tunneling configuration a clear oscillation of the phase coherence appears, as a result of the partial resynchronization of the quasiparticle oscillators (see also figure 3). The parameters adopted here are $J_\perp/\hbar = 5/(2\pi)$Hz, $\bar{\rho} = 50\ \mu$m^{-1}, ^{87}Rb mass, $g = g_{3D}/(2\pi l^2)$, with $l = \sqrt{\hbar/(m\Omega)}$, and $\Omega = 2\pi \times 2.1$ kHz.

with $\sigma_k^2(t)$ given by

$$\sigma_k^2(t) = \sigma^2 \cos^2(\omega_k t) + \left(\frac{\hbar^2}{M_k^2 \omega_k^2 \sigma^2}\right) \sin^2(\omega_k t). \tag{32}$$

Thus, during the time evolution, the standard deviations of the various modes evolve differently one from the other, since their frequencies ω_k and effective masses M_k are different.

The phase coherence of the system is quantified by the coherence factor [21, 23]

$$\mathcal{C}(t) = \langle\cos(\phi)\rangle_t = e^{-\frac{1}{2L^2}\sum_k \langle\phi_k^2\rangle_t} = e^{-\frac{1}{4L^2}\sum_k \sigma_k^2(t)} \tag{33}$$

where the averaging is calculated over the wavefunction at time t, namely $\Psi[\{\phi_k\}, t]$ in the ϕ_k representation, and the second equality holds for Gaussian distributed variables [21, 46]. As equation (33) shows, the coherence factor evolves in time as a function of the sum over all $\sigma_k^2(t)$. Depending on the specific form of the excitation spectrum ω_k and on the oscillator mass M_k, $\mathcal{C}(t)$ will show a different qualitative behavior. For non-tunneling parallel quasicondensates with a phononic spectrum, and a k-independent mass, the coherence factor decays exponentially to zero due to the dephasing of the modes [21]. The dephasing of $\mathcal{C}(t)$ is however absent in tunneling superfluids, where the nonzero tunneling energy J introduces a mass gap in the excitation spectrum [29]. This is exactly what happens in our case, as can be seen in the quasiparticle spectra of equations (17) and (27).

In the next subsections we will explicitly discuss our results for $\mathcal{C}(t)$, obtained in the side-by-side, and in the head-to-tail configurations. Before of that, let us briefly remind how the coherence factor is measured. In the experiments, after releasing the external potential which confines the quasicondensates, one can measure the distribution of the relative phase ϕ from the interference pattern between the subsystems. Knowing the relative phase profile allows to calculate the coherence factor of equation (33), by integrating $e^{i\phi}$ over the length of the imaging system [23, 45].

4.1. Side-by-side parallel quasicondensates

The phase coherence $\mathcal{C}(t)$ of side-by-side quasicondensates is shown in figure 2. It is obtained from equations (32) and (33) using the gapped Bogoliubov-like spectrum of equation (17), and the quasiparticle mass of equation (16). Differently from non-tunneling superfluids (orange dashed line), we find a clear rephasing phenomenon, which is more evident in longer systems (red line, $L = 100\,\mu$m) than in shorter ones (blue solid line, $L = 50\,\mu$m). We find that the oscillations of $\mathcal{C}(t)$ become more frequent and with higher amplitude if the atomic density $\bar{\rho}$ is increased. A similar behavior is obtained also if the value of $J_\perp$ is increased, signalling that the phase coherence is enhanced by a stronger tunneling between the subsystems.

The substructures around 2ms, and 4ms in the curves of figure 2 are due to the incoherent sum of the Gaussian standard deviations $\sigma_k^2(t)$, which appear at the exponential of the coherence factor $\mathcal{C}(t)$. This can be seen in figure 3, where we plot the normalized standard deviations $\sigma_k^2(t)/\sigma^2$ of the Gaussian wavefunctions $\Psi_k(\phi_k, t)$, for $k = \{0, 1, 2\}\pi/L$ (we use k instead of n with a slight abuse of notation). Due to the different quasiparticle energy $\hbar\omega_k$ for each mode, the deviations $\sigma_k^2(t)/\sigma^2$ oscillate with different frequencies, and with smaller amplitudes for larger values of k. The sum over all these modes produces the dephasing–rephasing oscillations shown in figure 2. This behavior of the system is completely different from that of uncoupled condensates, in which, since $\sigma_0^2(t) \propto t^2$ (orange dashed line of figure 3), the coherence factor decays exponentially to zero [21].
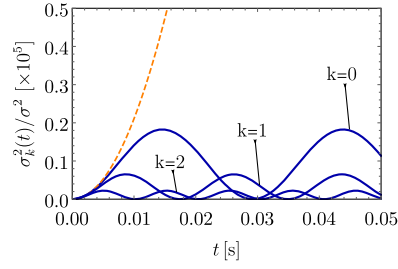
Figure 3. Time evolution of the Gaussian standard deviations $\sigma_k^2(t)$, rescaled with the σ^2 of the initial state, in the side-by-side configuration. In the absence of Josephson tunneling, the $\sigma_0^2(t)$ increases quadratically with time (orange dashed line), producing dephasing [17]. If tunneling occurs the mode $\sigma_0^2(t)$ does not diverge in time, and dephasing does not occur. Note that the modes here represented (blue solid lines) have different frequencies, and decreasing amplitudes for increasing $k = \{0, 1, 2\}\pi/L$. In this plot, we use the same parameters of the blue solid line in the previous figure.
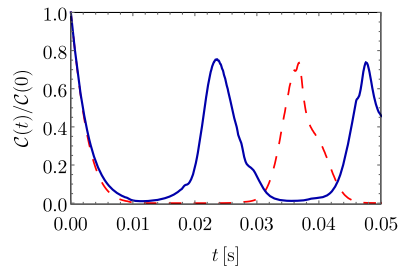

Figure 4. Oscillations of the coherence factor $\mathcal{C}(t)$ in head-to-tail parallel quasicondensates, where $J_\parallel/\hbar = 8/(2\pi)$Hz (blue solid line), and $J_\parallel/\hbar = 2/(2\pi)$Hz (red dashed line). Note that a higher value of the tunneling energy $J_\parallel$ enhances the frequency of the oscillations, and increases the overall coherence. The coherence factor is calculated by using equation (33), with the excitation spectrum ω_k given by the numerical solution of equation (23). For both curves, we use $L = 30\,\mu$m, $\bar{\rho} = 100\,\mu$m^{-1}, and the other parameters as in figure 2.

We point out that, following references [21, 29, 30], in the evaluation of the sum over the wavevectors k of equation (33) we have introduced a natural cutoff $\Lambda = \pi/\xi$, where $\xi = \hbar/\sqrt{mg\bar{\rho}}$ is the healing length. Considering that the $\sigma_k(t)$ strongly decrease in amplitude if k is increased, the cutoff does not introduce any spurious unphysical behavior.

We emphasize that, while our zero-temperature theory predicts the phase oscillations to continue indefinitely, a high phase coherence cannot be observed in the experiments for very long times. This is due to the intrinsic presence of thermal excitations, and the conditions under which our theory is valid are highlighted in the conclusions.

4.2. Head-to-tail parallel quasicondensates

The low-energy excitation spectrum of head-to-tail parallel superfluids, equation (27), is qualitatively similar to that of side-by-side ones, equation (17). Due to this formal analogy, we expect to observe a similar qualitative picture in the relative phase dynamics of the system. Indeed, after a sudden coupling of the quasicondensates with a delta-like Josephson junction with tunneling energy $J_\parallel$, the coherence factor $\mathcal{C}(t)$ of equation (33) oscillates in time. As in the previous section, the oscillation is a result of the partial dephasing and rephasing of the quasiparticle modes. In figure 4 we plot $\mathcal{C}(t)$ as a function of time for different tunneling energies: $J_\parallel/\hbar = 8/(2\pi)$Hz (blue solid line) and $J_\parallel/\hbar = 2/(2\pi)$Hz (red dashed line). Thus, for higher values of $J_\parallel$ the oscillations of $\mathcal{C}(t)$ are more frequent, and with a higher baseline, signalling a higher phase coherence. As we stress in the conclusions, and similarly to the case of head-to-tail quasicondensates, our zero-temperature approach does not describe the thermal decoherence processes which could dissipate these oscillations at long times. Thus, in the experiments, a sufficiently high value of $J_\parallel$ is needed, to observe the phase oscillations before of the onset of thermal dephasing.

Let us finally note that a single quasicondensate can be split into a couple of parallel head-to-tail superfluids by superimposing an optical potential to the longitudinal magnetic trap [47]. The tunability of this configuration and the possibility to engineer a box-like potential along x are useful tools to satisfy the hypothesis of a constant density $\bar{\rho}$, and to implement our open boundary conditions.

5. Conclusions

We have derived the excitation spectrum of tunneling quasicondensates in two distinct experimental configurations: side-by-side, and head-to-tail superfluids. We find that the sudden coupling of the independent quasicondensates produces an interesting nonequilibrium dynamics of the relative phase between the subsystems. In both system configurations, due to the formal similarities in the excitation spectrum, the coherence factor oscillates in time, driven by a nonzero tunneling between the quasicondensates. The coherence and the frequency of the oscillations are enhanced for higher atomic densities and for higher tunneling energies.

The unavoidable thermal fluctuations of temperature T setup a typical time τ above which our zero-temperature results are no more reliable and a thermal-induced dephasing is expected. The microscopic source of the decoherence is the coupling between the center of mass modes, constituting a thermal bath, and the collective modes of the relative phase [17]. We estimate the typical time τ as $\tau = \hbar/(k_B T)$, where k_B is the Boltzmann constant [17]. Thus, our analytical and numerical dynamical results become unreliable for a time duration t such that $t \gg \tau$. Considering this criterion, the experimental observation of the phase oscillations shown in figures 2, and 4, requires that the temperature before the splitting is in the nK range. Indeed, assuming that the oscillations are dissipated only in part on a time interval up to 10τ, an initial temperature of 5nK would allow to observe 15ms of the dynamics. By properly tuning the tunneling energy, this time should be sufficient to observe at least a partial rephasing of the system.

We are fully aware that reaching these conditions of temperature in our setup poses a real experimental challenge, since analogous experiments in atom chips are currently performed at a temperature of 18nK [31]. At the same time, considering the huge experimental developments of the last decades, we believe that the implementation of these experimental conditions will be soon technically feasible.

ORCID iDs

A Tononi ⓘ https://orcid.org/0000-0002-0023-3977
S Wimberger ⓘ https://orcid.org/0000-0002-8433-1733
A Cappellaro ⓘ https://orcid.org/0000-0001-6110-2359
L Salasnich ⓘ https://orcid.org/0000-0003-0817-4753

References

[1]   Anderson M H, Ensher J R, Matthews M R, Wieman C E and Cornell E A 1995 *Science* **269** 5221
[2]   Davis K B, Mewes M-O, Andrews M R, van Druten N J, Durfee D S, Kurn D M and Ketterle W 1995 *Phys. Rev. Lett.* **75** 3969
[3]   Streltsov A, Adesso G and Plenio M 2017 *Rev. Mod. Phys.* **89** 041003
[4]   Pezzé L, Smerzi A, Oberthaler M K, Schmied R and Treutlein P 2018 *Rev. Mod. Phys.* **90** 035005
[5]   Giampaolo S M, Trombettoni A, Krüger P and Macrí T 2018 *Phys. Rev. A* **97** 041602
[6]   Anderson P W 1986 *The Lesson of Quantum Theory* ed J D E de Boer and O Ulfbeck (Amsterdam: Elsevier)
[7]   Leggett A J and Sols F 1991 *Found. Phys.* **21** 353
[8]   Castin Y and Jean Dalibard J 1997 *Phys. Rev. A* **55** 4330
[9]   Zapata I, Sols F and Leggett A J 1998 *Phys. Rev. A* **57** 28(R)
[10] Villain P, Lewenstein M, Dum R, Castin Y, You L, Imamoglu A and Kennedy T A B 1999 *J. Mod. Opt.* **44** 1775
[11] Zapata I Sols F and Leggett A J 2003 *Phys. Rev. A* **67** 021603(R)
[12] Folman R, Krüger P, Cassettari D, Hessmo B, Maier T and Schmiedmayer J 2000 *Phys. Rev. Lett.* **84** 4749
[13] Cronin A D, Schmiedmayer J and Pritchard D E 2009 *Rev. Mod. Phys.* **81** 1051
[14] Zobay O and Garraway B M 2001 *Phys. Rev. Lett.* **86** 1195
[15] Schumm T, Hofferberth S, Andersson L, Wildermuth S, Groth S, Bar-Joseph I, Schmiedmayer J and Krüger P 2005 *Nat. Phys.* **1** 57
[16] Polkovnikov A, Altman E and Demler E 2006 *Proc. Natl Acad. Sci. USA* **103** 6125
[17] Burkov A A, Lukin M D and Demler E 2007 *Phys. Rev. Lett.* **98** 200404
[18] Gritsev V, Altman E, Demler E and Polkovnikov A 2006 *Nat. Phys.* **2** 705
[19] Shin Y, Saba M, Pasquini T A, Ketterle W, Pritchard D E and Leanhardt A E 2004 *Phys. Rev. Lett.* **92** 050405

[20] Shin Y, Sanner C, Jo G-B, Pasquini T A, Saba M, Ketterle W, Pritchard D E, Vengalattore M and Prentiss M 2005 *Phys. Rev. A* **72** 021604(R)
[21] Bistritzer R and Altman E E 2007 *Proc. Natl Acad. Sci. USA* **104** 9955
[22] Altman E 2012 Non equilibrium quantum dynamics in ultra-cold quantum gases *Strongly Interacting Quantum Systems Out of Equilibrium* (Lecture Notes of the Les Houches Summer School vol 99) (https://doi.org/10.1093/acprof:oso/9780198768166.003.0001)
[23] Hofferberth S, Lesanovsky I, Fischer B, Schumm T and Schmiedmayer J 2007 *Nature* **449** 324
[24] Berges J, Borsányi S and Wetterich C 2004 *Phys. Rev. Lett.* **93** 142002
[25] Gring M *et al* 2012 *Science* **337** 1318
[26] Langen T, Geiger R, Kuhnert M, Rauer B and Schmiedmayer J 2013 *Nat. Phys.* **9** 640
[27] Langen T *et al* 2015 *Science* **348** 207
[28] Dalla Torre E G, Demler E and Polkovnikov A 2013 *Phys. Rev. Lett.* **110** 090404
[29] Foini L and Giamarchi T 2017 *Eur. Phys. J.: Spec. Top.* **226** 2763
[30] Foini L and Giamarchi T 2015 *Phys. Rev. A* **91** 023627
[31] Pigneur M, Berrada T, Bonneau M, Schumm T, Demler E and Schmiedmayer J 2018 *Phys. Rev. Lett.* **120** 173601
[32] van Nieuwkerk Y D and Essler F H L 2019 *J. Stat. Mech.* 084012
[33] van Nieuwkerk Y D and Essler F H L 2020 in preparation
[34] Polo J, Ahufinger V, Hekking F W J and Minguzzi A 2018 *Phys. Rev. Lett.* **121** 090404
[35] Salasnich L, Parola A and Reatto L 2002 *Phys. Rev. A* **65** 043614
[36] Popov V N 1972 *Theor. Math. Phys.* **11** 565
[37] Betz T *et al* 2011 *Phys. Rev. Lett.* **106** 020407
[38] Son D T and Stephanov M A 2002 *Phys. Rev. A* **65** 063621
[39] Gallemí A, Pitaevskii L P, Stringari S and Recati A 2019 *Phys. Rev. A* **100** 023607
[40] Josephson B D 1962 *Phys. Lett.* **1** 251
[41] Smerzi A, Fantoni S, Giovanazzi S and Shenoy S R 1997 *Phys. Rev. Lett.* **79** 4950
[42] Bogoliubov N N 1947 *J. Phys. (USSR)* **11** 23
[43] Atkinson D A and Crater H W 1975 *Am. J. Phys.* **43** 301
[44] Robinett R W 2004 *Found. Phys. Lett.* **17** 607
[45] van Nieuwkerk Y D, Schmiedmayer J and Essler F H L 2018 *SciPost Phys.* **5** 046
[46] Kardar M 2004 *Statistical Physics of Fields* (Cambridge: Cambridge University Press)
[47] Tajik M, Rauer B, Schweigler T, Cataldini F, Sabino J, Møller F S, Ji S-C, Mazets I E and Schmiedmayer J 2019 *Opt. Express* **27** 33474